Fast Biofluid Transport of High Conductive Liquids Using AC Electrothermal Phenomenon, A Study on Substrate Characteristics

A. Salari, C. Dalton
Department of Electrical & Computer Engineering, University of Calgary, Calgary, AB, Canada

Abstract: Electrokinetic micropumps are widely used in biomedical and lab-on-a-chip applications. In this paper, AC electrothermal (ACET) micropump with two arrays of microelectrodes are simulated, and different substrate material and thicknesses are investigated using COMSOL Multiphysics. The results show that glass substrates more efficiently pump the electrolyte solution compared to silicon substrates. Also, thicker substrates are more beneficial than thinner ones. Therefore, well-chosen substrate parameters can provide potential techniques for high flow rate ACET micropumping.

Keywords: AC electrothermal, Biofluid, High flow rate.

1. Introduction

Electrokinetics has many applications in a wide range of areas, such as lab-on-a-chip and biomedical microdevices. The electrothermal effect has been used for biofluid delivery systems since it has high pumping efficiency for high conductive liquids (>0.1 S/m) compared to other electrokinetic techniques such as electroosmosis. AC electrothermal (ACET) micropumps are based on the temperature gradient caused by Joule heating or an external heat source, which generates permittivity and conductivity gradients in the bulk of the liquid. When the liquid is subjected to an electric field, the ACET force is created. Several parameters govern the phenomenon. Some of them have been studied in the literature including actuation voltage and frequency [1], planar electrode geometry [2], number of electrodes [3], and non-planar electrodes [4].

In this paper, the effect of substrate material and thickness are numerically investigated. Two commonly used materials, glass and silicon, are employed and the resultant electric field, temperature distribution, and fluid flows are illustrated.

2. Theory

Electrothermal effect is a multiphysics phenomenon containing electrostatics, heat transfer, and fluid dynamics, each of which are elaborated on in the following subsections. By energizing an array of microelectrodes placed in contact with an electrolyte solution, an electric field is generated in the solution, which causes Joule heating in the system. This can cause conductivity and permittivity gradients, which in turn, introduces electrothermal force throughout the solution and fluid flow is generated.

2.1 Electrostatics

Applying an AC electric voltage to an electrode causes an electric field to be generated throughout the medium in which the electrodes are positioned. Laplace's equation can be used to determine the electric potential V in a homogeneous medium:

$$\nabla^2 V = 0 \quad (1)$$

Electric displacement field D can then be calculated as:

$$E = -\nabla V \quad (2)$$

$$D = \varepsilon E \quad (3)$$

where E and ε are electric field and permittivity of the medium, respectively.

Moreover, mobile charge density can be written as [4]:

$$\rho = \nabla\varepsilon \cdot E + \varepsilon \nabla \cdot E \quad (4)$$

2.2 Heat Transfer

Electric field distribution throughout the system, which causes Joule heating as a heat source, can be determined by applying the energy balance equation [5]:

$$k\nabla^2 T + \frac{1}{2}\langle \sigma E^2 \rangle = 0 \quad (5)$$

where k, T, and σ are thermal conductivity coefficient, temperature field, and electrical conductivity, respectively. $\frac{1}{2}\langle \sigma E^2 \rangle$ is the Joule heating as the heat source.

For the case of asymmetric microelectrodes, the resultant E is non-uniform, causing a spatial

variation in heat transfer and consequently spatial gradient in local conductivity and permittivity as:

$$\nabla\varepsilon = \left(\frac{\partial\varepsilon}{\partial T}\right)\nabla T \quad (6)$$

$$\nabla\sigma = \left(\frac{\partial\sigma}{\partial T}\right)\nabla T \quad (7)$$

For aqueous solutions and temperature around 293 ˚K, permittivity and electrical conductivity can be expressed as [6]:

$$\left(\frac{1}{\varepsilon}\right)\left(\frac{\partial\varepsilon}{\partial T}\right) \approx -0.004 \quad (8)$$

$$\left(\frac{1}{\sigma}\right)\left(\frac{\partial\sigma}{\partial T}\right) \approx 0.02 \quad (9)$$

2.3 Fluid Dynamics

Applying Navier-Stokes equations for an incompressible fluid flow of low Reynolds number in the presence of electrothermal force $\langle F_{et}\rangle$ as a body force one can write:

$$-\nabla p + \eta\nabla^2\boldsymbol{u} + \langle F_{et}\rangle = 0 \quad (10)$$

$$\nabla.\boldsymbol{u} = 0 \quad (11)$$

where p, η, and $\boldsymbol{u}$ are pressure, fluid viscosity, and velocity field vector. $\langle F_{et}\rangle$ can be expressed as:

$$\langle F_{et}\rangle = -\left[\frac{1}{2}\left(\frac{\nabla\sigma}{\sigma} - \frac{\nabla\varepsilon}{\varepsilon}\right)E\cdot\frac{\varepsilon E}{1+(\omega\tau)^2} + \frac{1}{2}\nabla\varepsilon|E|^2\right] \quad (12)$$

where ω and τ are angular frequency and charge relaxation time, respectively.

3. Use of COMSOL Multiphysics

In this paper, the effects of substrate thickness and material for two rows of microelectrodes placed on the top and bottom of a fluidic microchannel in an ACET micropump are studied. Heat transfer is an important phenomenon in ACET micropumps. Therefore thermal characteristics of the substrates can dramatically affect the pumping efficiency. Numerical investigation was employed for simulating different combinations of silicon and glass substrates. 2D simulation of an ACET micropump (Figure 1) was performed using finite element software COMSOL Multiphysics.

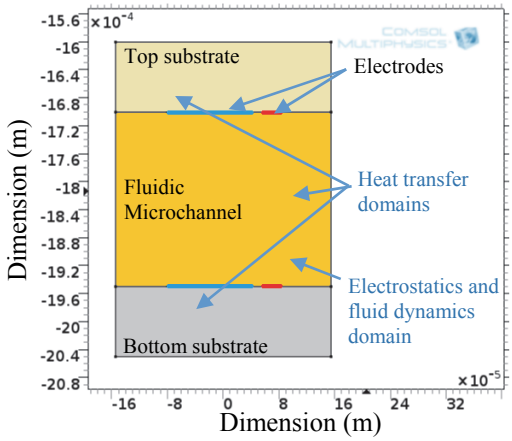

Figure. 1 The ACET micropump geometry

3.1 Electrostatics Module

Electric field distribution along the microchannel shown in Figure 1 was obtained assuming two pairs of coplanar asymmetric microelectrodes, in which the thin electrode was at 7 Vrms, and the wide electrode was grounded. Actuation frequency was kept constant at 100 kHz. Periodic boundary conditions were assigned for side boundaries (right and left boundaries in Figure 1) representing the rest of the electrodes. Zero charge conditions were assigned for the area inside the microchannel not covered by microelectrodes. Electrolyte solution with $\sigma = 0.224\ S/m$ was used.

3.2 Heat Transfer Module

Heat transfer through the bulk of the fluid and substrates were determined assuming glass ($k = 1.1\ W/mK$) and silicon ($k = 131\ W/mK$) as the substrate material and $k = 0.6\ W/mK$ for the electrolyte solution. Periodic boundary conditions were applied for the right and left domains' boundaries. The temperature of substrate outer boundaries were assumed at ambient temperature (T=293° K).

3.3 Laminar Flow Module

Laminar flow with electrothermal force as the external body force was performed for the electrolyte solution with a temperature dependent viscosity, and periodic boundary conditions on right and left boundaries of the domain. No-slip condition on walls was applied for the fluidic microchannel walls.

4. Results

Figure 2 shows the potential and electric field distributions throughout the fluidic microchannel. As shown, the maximum electric field occurs near the thin electrode inside the bulk of the electrolyte solution. Therefore, maximum Joule heating is generated at this area causing the temperature increases correspondingly.

Figure 3 shows the temperature distribution in the whole device for ACET micropumps with three different configurations of material substrates which are silicon-silicon, glass-glass, and silicon-glass. As the thermal conductivity of glass is much lower than silicon, heat generated in the bulk of the fluid encounters more resistance dissipating to the ambient. As a result, maximum temperature in the micropump for the case of glass substrates, which is ≈299 °K, is higher than the one of silicon substrate, which is ≈295 °K.

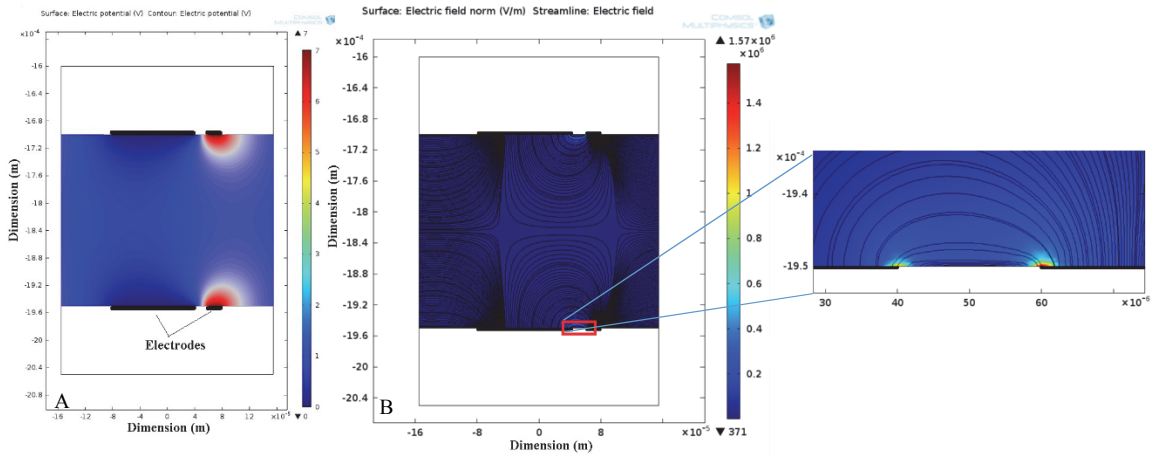

Figure 2. (A) Potential distribution and (B) electric field distribution for the ACET micropump. The highest electric field gradient occurs near the thin electrode as the potential approaches 7 V, while it is almost zero near the wide one. As the similar voltages are applied to top and bottom microelectrodes, the electric and potential fields are vertically symmetrical.

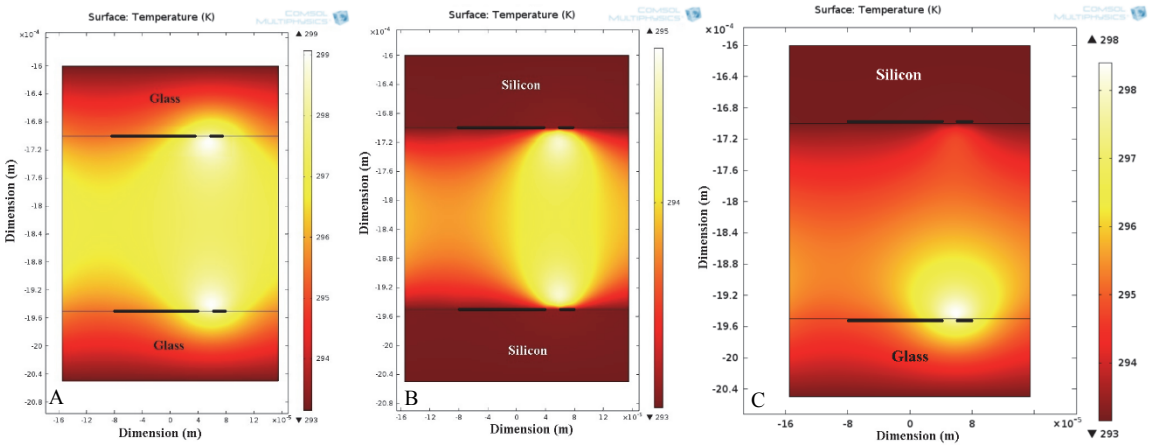

Figure 3. Temperature distribution for three different substrate material configurations; (A): glass-glass; (B): silicon-silicon; (C): silicon-glass. Higher thermal conductivity of silicon causes it to sustain negligible temperature gradient, while ≈5 °K temperature drop is observed in glass substrate.

Figure 2 also shows that the maximum gradient of electric field occurs near the thin electrode, meaning that the strongest electrothermal force is generated at this area. This predicts that the maximum ACET velocities will be in the same area.

A comparison between micropumps with different substrate thicknesses is depicted in Figure 4. As thicker substrates induce higher thermal resistance for heat dissipation, micropumps with 1000 µm thick substrates can generate higher flow rates up to 12% than 100 µm thick ones.

Figure 5 shows the resultant ACET fluid flow for the micropumps with four different configurations. It illustrates that maximum flow rates in each configuration occur near the thin electrode surfaces. The results show that using glass substrates can increase the ACET flow velocity up to 230 µm/s at the height of ~10 µm above the electrode surface compared to 113 µm/s for silicon substrates at the same height, which means that almost 200% increase in ACET velocity is achieved.

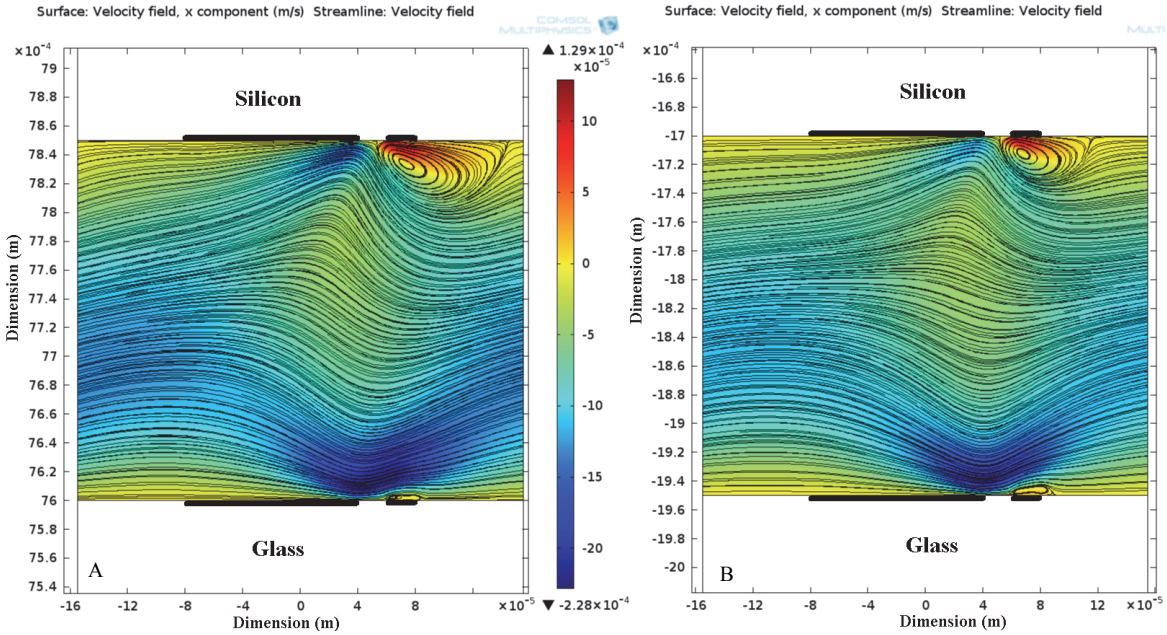

Figure 4. ACET fluid flow for two different silicon-glass substrate thicknesses; (A): 1000 µm; (B): 100 µm. Thicker substrates provide higher flow rates than thinner ones. Also, as it was expected maximum ACET velocity (x-component) occurs near the glass substrates.

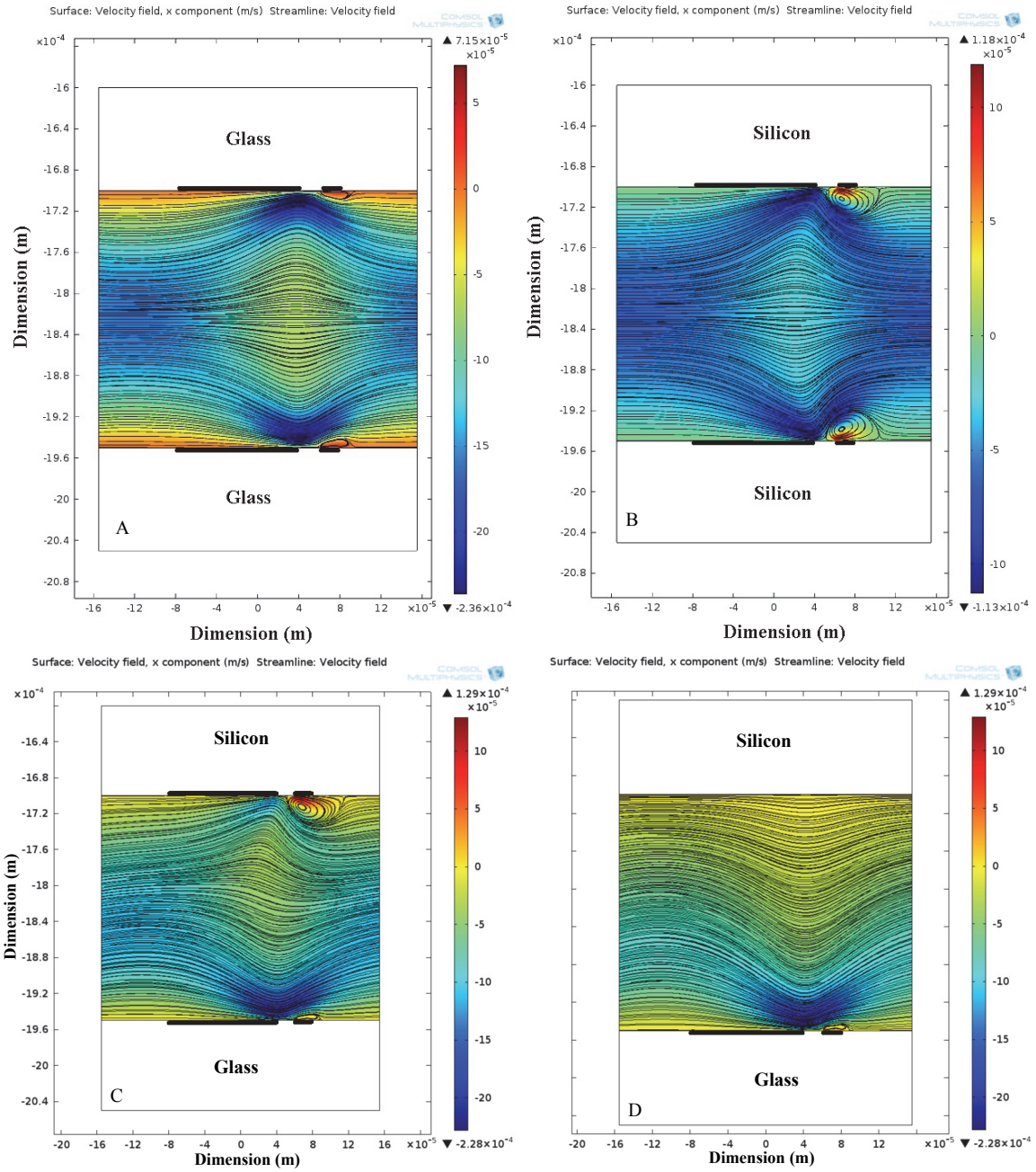

Figure 5. ACET fluid flow for four different ACET micropump configurations; different substrate materials used as (A): glass-glass, (B): silicon-silicon, and (C): silicon-glass. (D): shows a micropump with one array of microelectrodes placed at the bottom of the fluidic microchannel. Glass-glass configuration provides the highest flow rates than the others. Also, maximum ACET velocity (x-component) occurs near the electrodes' edge. Moreover, net flow generated near the glass substrates suppresses the ACET vortices formed on top of the thin electrodes. This does not happen for the vortices near silicon substrates, as the net flow at this area has less strength.

5. Conclusions

In this paper, ACET micropump with two microelectrode arrays on top and the bottom of the fluidic microchannel with different substrate materials was investigated. Fluid flow simulation of such micropumps showed that substrate materials with lower thermal conductivity can increase the pumping flow rate, but do so at a cost of increasing the fluid temperature. Also, thicker substrates can decrease the heat transfer rate and consequently increase the flow rate. Choosing such parameters carefully can be a potential technique in achieving higher flow rates in electrokinetic based fluid transport systems.

6. References

1. R. Zhang, C. Dalton and G. A. Jullien, "Two-phase AC Electrothermal Fluidic Pumping in a Coplanar Asymmetric Electrode Array," *Microfluid. Nanofluid.,* 10, 521-529 (2011).
2. Q. Yuan, K. Yang and J. Wu, "Optimization of Planar Interdigitated Microelectrode Array for Biofluid Transport by AC Electrothermal Effect," *Microfluid. Nanofluid.,* 16, 167-178 (2014).
3. A. Salari, M. Navi and C. Dalton, "AC Electrothermal Micropump for Biofluidic Applications Using Numerous Microelectrode Pairs," in *IEEE Conference on Electrical Insulation and Dielectric Phenomena*, Des Moines, IA (2014).
4. E. Du and S. Manoochehri, "Microfluidic Pumping Optimization in Microgrooved Channels with AC Electrothermal Actuations," *Applied Physics Letters,* 96, 034102 1-3 (2010).
5. M. Lian, N. Islam and J. Wu, "AC Electrothermal Manipulation of Conductive Fluids and Particles for Lab-Chip Applications," *IET Nanobiotechnol.,* 1, 36-43 (2007).
6. M. Sigurdson, C. D. Meinhart and H. C. Feidman, "AC Electrothermal Enhancement of Heterogeneous Assays in Microfluidics," *Lab Chip,* **7**, 1553-1559 (2007).

7. Acknowledgements

The authors would like to acknowledge the financial support received from Natural Sciences and Engineering Research Council (NSERC), and also software platform provided by COMSOL Inc. and CMC Microsystems.